Xenophobic dark matter

David Sanford

Citation: AIP Conference Proceedings **1604**, 91 (2014); doi: 10.1063/1.4883416
View online: http://dx.doi.org/10.1063/1.4883416
View Table of Contents: http://scitation.aip.org/content/aip/proceeding/aipcp/1604?ver=pdfcov
Published by the AIP Publishing

Xenophobic Dark Matter

David Sanford

California Institute of Technology, Pasadena, CA 91125, USA

Abstract. We describe models in which dark matter is xenophobic, with significantly reduced signal strength in direct detection experiments using xenon as a target material. Such models alleviate tension between xenon-based constraints and possible signal at other direct detection experiments, and in particular regions of interest at CoGeNT and CDMS are largely below XENON100 bounds in the purely xenophobic limit. We also show the constraints from upcoming LUX results and orthogonal searches using Fermi-LAT results from line searches in dwarf spheroidals and monojet searches at CMS.

Keywords: Dark matter
PACS: 95.35.+d

INTRODUCTION

Recent progress in the sensitivity of dark matter (DM) direct detection experiments has been substantial, with multiple experiments improving sensitivities by orders of magnitude in the past few years. In particular, a number of contradictory results in the light mass window have garnered significant interest. Potential signals have been found at the DAMA [1], CoGeNT [2], CRESST [3], and CDMS-Si [4] experiments, all consistent with light weakly interacting massive particles (WIMPs) with masses of $\mathcal{O}(10\ \text{GeV})$ and spin-independent (SI) cross-section of $\mathcal{O}(10^{-6} - 10^{-3}\ \text{pb})$ under typical theory assumptions. However, none of these signals are fully consistent under these assumptions, and moreover are strongly constrained by limits at CDMS-Ge detectors [5, 6], Edelweiss [7], XENON10 [8], and XENON100 [9, 10].

The conflicting experimental situation has led to a variety of attempts to reconcile results. The original attempt to explain the DAMA experiment in the face of other results is inelastic DM [11], though such models are no longer viable in their simplest form. Experimental considerations such as the effective scintillation light yield ($\mathscr{L}_{\text{eff}}$) [12] and channeling in sodium-iodide at DAMA [13, 14] have also been put forward to explain inconsistencies, and the possibility of other unknown systematic effects remains a known issue. Uncertainties in the DM velocity distribution in the galaxy has also been shown to have a significant effect on direct detection results [15, 16, 17], possibly resolving some discrepancies.

Here we instead focus on the simple particle physics of isospin-violating dark matter (IVDM) [18, 19, 20, 21, 22], in which the coupling of DM to protons and neutrons are unequal and generically unrelated. IVDM is the natural general theory of DM on the nucleon level, and is exhibited by various DM interactions with the Standard Model (SM), including Z-mediated interactions, interaction through dark photons with kinetic mixing, and new scalar and fermionic mediators. Indeed, the assumption of isospin-invariance for spin-independent results is an artifact of interest in Higgs-mediated neutralino scattering. We consider a range of possible neutron-to-proton coupling rations f_n/f_p, but focus on models with $f_n/f_p \sim -0.7$, which is phenomenologically preferred due to reduced sensitivity at the xenon-based experiments which currently possess the strongest limits on DM direct detection.

ISOSPIN-VIOLATING DARK MATTER

For DM particles of mass $\mathcal{O}(10)$ GeV interacting with nuclei at typical galactic velocities, the characteristic momentum transfer is $\mathcal{O}(1\ \text{keV})$. This is far too small to resolve the internal structure of the nucleon, and only partially resolves the internal structure of the nucleus itself. It is therefore natural in direct detection experiments to consider only the effective coupling of DM to protons and neutrons, denoted here by f_p and f_n for SI scattering. The case of $f_n = f_p$ dominates the direct detection literature, approximating the situation in which DM couples to quarks through Higgs boson exchange; in this case there is a well-known A^2 enhancement due to constructive interference which improves sensitivity for heavier elements in direct detection experiments.

Workshop on Dark Matter, Neutrino Physics and Astrophysics CETUP 2013*
AIP Conf. Proc. 1604, 91-97 (2014); doi: 10.1063/1.4883416

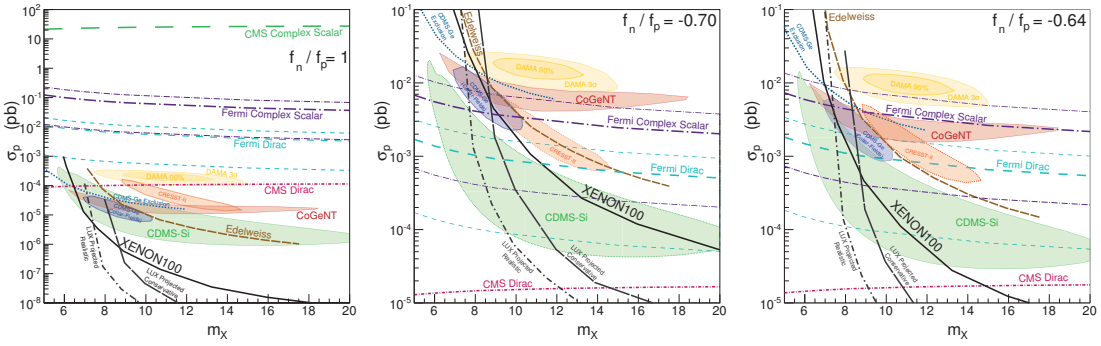

FIGURE 1. *Regions of interest and exclusion contours in the* (m_X, σ_p) *for neutron-to-proton coupling ratios* $f_n/f_p = 1$ *(left),* $f_n/f_p = -0.70$ *(center) and* $f_n/f_p = -0.64$ *(right).* Plotted are the 90% CL ROIs for CDMS-Si [4], CoGeNT [2], and CDMS-Ge (Collar/Fields) [23], the 90% and 3σ ROIs for DAMA [1] as determined in Refs. [24, 25], and exclusion contours from XENON100 [9, 10], Edelweiss [7], and CDMS [6]. Also plotted are 90% CL exclusion contours from CMS and from the Fermi-LAT, assuming DM is either a complex scalar or Dirac fermion coupling only to first generation quarks through an effective contact interaction permitting unsuppressed spin-independent scattering and *S*-wave annihilation. The thin dot-dashed violet and dashed teal lines correspond to the systematic uncertainty in the Fermi-LAT bounds from astrophysical uncertainties for complex scalar and Dirac fermion candidates, respectively.

However, the ratio f_n/f_p can take a multitude of values in different DM frameworks, and may even be a free parameter depending on the model. Both dark photon and Z-mediated models are located at specific values of $f_n \neq f_p$, while models with a new s- or t-channel mediator can possess any value of f_n/f_p based on couplings. In particular, for $-1.5 \lesssim f_n/f_p \lesssim -0.5$, the cross-section for scattering off nuclei is severely reduced relative to typical $f_n = f_p$ determinations due to destructive interference. This in turn significantly alters the results of direct detections experiments. The true physical quantity reported by such experiments is the "normalized to nucleon" DM scattering cross-section,

$$\sigma_N^Z = (\hat{\sigma}_A/A^2) \times (\mu_p^2/\mu_A^2), \tag{1}$$

where $\hat{\sigma}_A$ is the zero momentum transfer scattering cross-section off a nucleus, Z is the atomic number, A is the atomic weight, and μ_p and μ_A are the reduced masses of the DM-proton and DM-nucleus systems respectively. However, direct detection experiments typically refer to the reported quantity as the "DM-proton scattering cross-section", σ_p. While the quantities are identical for $f_n = f_p$, and in that case $\sigma_n \approx \sigma_p$ as well, they can diverge drastically for a more general ratio of couplings.

Further complicating the reported results of direct detection experiments is the existence of multiple isotopes for some detector materials. In such cases the reported value becomes a weighted average of the normalized to nucleon cross-sections for all isotopes present in the detector (typically simply natural abundances), with relations to the true DM-nucleon scattering cross-section of

$$D_p^Z \equiv \frac{\sigma_N^Z}{\sigma_p} = \frac{\sum_i \eta_i \mu_{A_i}^2 [Z + (f_n/f_p)(A_i - Z)]^2}{\sum_i \eta_i \mu_{A_i}^2 A_i^2} \tag{2}$$

$$D_n^Z \equiv \frac{\sigma_N^Z}{\sigma_n} = D_p^Z \left(\frac{f_p}{f_n}\right)^2. \tag{3}$$

This effect prevents vanishing cross-sections for elements with multiple isotopes, as complete destructive interference in one isotope will result in incompletely suppressed cross-sections in other isotopes. In particular, the point of "maximal xenophobia" – maximally suppressed cross-section for scattering off xenon – occurs for a coupling ratio $f_n/f_p = -0.7$.

Fig. 1 shows current limits and regions of interest (ROIs), along with the projected sensitivity of LUX [26], for various values of f_n/f_p. The typical case of $f_n/f_p = 1$ is considered as a baseline, along with maximal xenophobic case of $f_n/f_p = -0.7$ and the somewhat less xenophobic case of $f_n/f_p = -0.64$. For both xenophobic cases the values of σ_p associated with all direct detection experiments is enhanced significantly due to the general destructive interference.

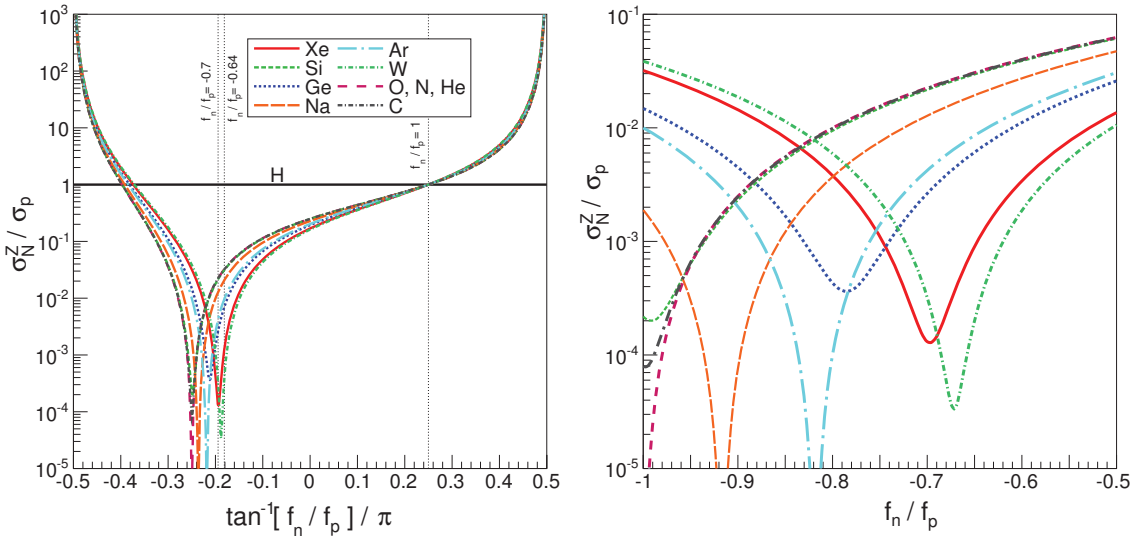

FIGURE 2. *Ratio of the normalized-to-nucleon cross section reported by direct detection experiments to the true nucleon cross section.* Results are shown for $\sigma_N^Z/\sigma_p = D_p^Z$ as a function of f_n/f_p for various elements. The entire range of f_n/f_p is shown (top) as well as the xenophobic region (bottom). All plots assume $m_X = 8$ GeV, but are highly insensitive to this choice.

For $f_n/f_p = 1$ current XENON100 bounds tightly constrain all possible signals over the entire range of viable masses. For $f_n/f_p = -0.7$ the constraints weaken considerably, with the reported CDMS-Si ROI almost entirely avoiding XENON100 bounds, and the CoGeNT ROI (as well as a ROI corresponding to a reanalysis CDMS-Ge by Collar and Fields [23]) remaining below the XENON100 bounds for $m_X \lesssim 9$ GeV. For $f_n/f_p = -0.64$ the constraints on all three ROIs from XENON100 are stronger, but portions of all three ROIs remain below the XENON100 bounds for $m_X \lesssim 9$ GeV and the overlap between the CDMS-Si and CoGeNT/CDMS-Ge (Collar-Fields) ROIs is improved. In both cases the CRESST-II and DAMA ROIs remain above the XENON100 limit. LUX projected sensitivity has significant power to further constrain current ROIs, though it does not completely due to conservative scintillation threshold cuts [26] a portion of the ROIs remain below LUX sensitivity.

Fig. 2 shows the value of the ratio D_p^Z for various values of f_n/f_p for $m_X = 8$ GeV (though mass dependence is very weak). By definition $D_p^Z = 1$ for $f_n/f_p = 1$, while $D_p^Z \to \infty$ for $f_p \to 0$ as proton scattering vanishes but neutron scattering can still occur. A significant degree of destructive interference is present for $-3 \lesssim f_n/f_p \lesssim 0$, with $D_p^Z \lesssim 10^{-2}$ in at least some elements for $-1.5 \lesssim f_n/f_p \lesssim -0.5$. For elements with only one naturally-abundant isotope, as with {O, N, He, Na, Ar} shown here, complete destructive interference is possible and $D_p^Z \to 0$ for $f_n/f_p \to -Z/(A-Z)$. For elements with multiple naturally abundant isotopes D_p^Z has a minimum in the range $3 \times 10^{-5} - 5 \times 10^{-4}$ based on the element in question. Similar behavior holds for D_n^Z (not shown), except that $D_n^Z \to \infty$ for $f_n/f_p \to 0$ due to vanishing neutron coupling.

The relative enhancement or suppression of normalized to nucleon cross-section in a given element relative to xenon, σ_N^Z/σ_N^{Xe} is shown explicitly in Fig. 3. For most of the range of f_n/f_p the ratio is close to unity, only diverging from unity in the destructive interference region. This is reflective of the fact that $A \sim Z$ is roughly true for all elements besides hydrogen, so large sensitivity ratios can only occur near points of severe destructive interference for one element. The maximum enhancement differs from element to element due to differing proton-to-neutron ratios, with greater enhancement for ratios further from xenon. Focusing on the elements relevant to the CoGeNT and CDMS ROIs, the maximal enhancement in silicon is ~ 200 while the maximum enhancement in germanium is ~ 25, which contributes to the fact that the CDMS-Si ROI is able to completely evade XENON100 bounds for maximal xenophobia while the CoGeNT/CDMS-Ge (Collar-Fields) ROIs are only partially below the XENON100 limit. Conversely, the maximal enhancement of sodium relative to xenon is ~ 100, resulting in the DAMA 90% region lying at least a factor of five above the XENON100 limit across its mass range even for maximal xenophobia.

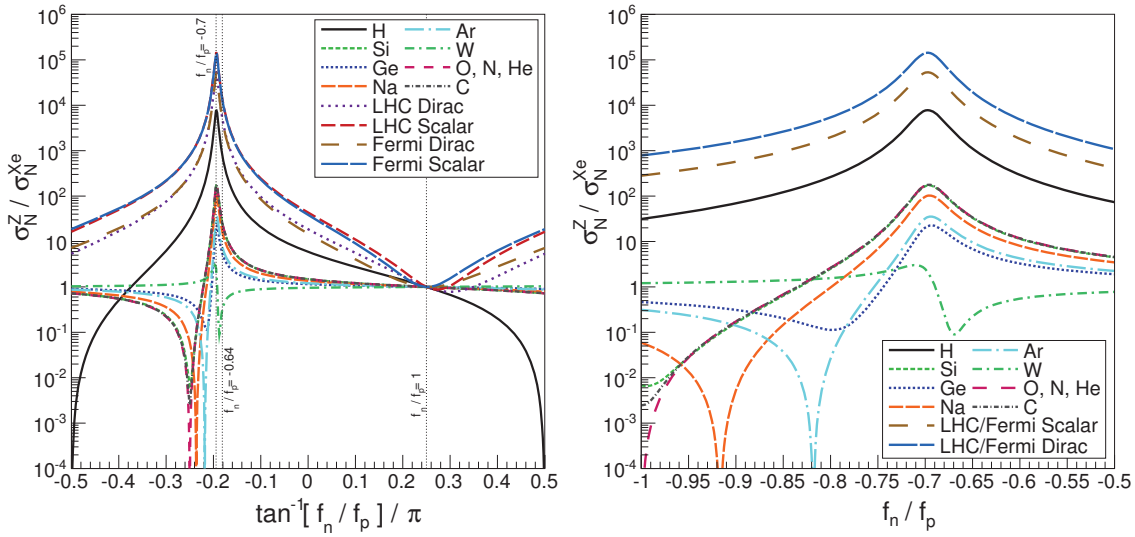

FIGURE 3. *Ratio of σ_N^Z in various experiments to σ_N^{Xe}.* Results are shown as a function of f_n/f_p for scattering off various elements, as well as for LHC and Fermi determinations. In the xenophobic region the behavior of LHC and Fermi bounds for a given operator are visually identical.

INDIRECT DETECTION AND COLLIDER SEARCHES

One of the cornerstones of the WIMP paradigm is detectability on multiple frontiers, as the same interactions which produce viable direct detection signals generically also have viable indirect detection and collider signals. Dark matter interactions with quarks imply baryon and photon signals for indirect searches, while at colliders various probes are available on a model-dependent basis, such as searches involving missing energy and a single jet, photon, or W/Z boson, dijet resonance searches, and searches for t-channel mediators similar to squark searches. Such searches are especially important for models with destructive interference between protons and neutrons, where bounds from indirect searches and colliders are stronger relative to the isospin-invariant case.

However, interpreting indirect and collider search limits in the direct detection plane proves non-trivial. There exists a significant model dependence, requiring assumptions about the coupling structure and mediator particle mass to compare searches in different regimes. Moreover, there is a significant degeneracy in mapping the underlying couplings to individual quarks into just the parameters f_p and f_n that define spin-independent direct detection. These considerations can result in variations of orders of magnitude in the direct detection cross-section inferred from indirect and collider searches.

Here we consider an effective operator approach for comparison of results, choosing only operators which produce s-wave annihilation and no velocity suppression in direct detection scattering. The former condition is imposed to allow for meaningful bounds from indirect detection experiments. while the latter removes models for which direct detection cross-sections consistent with existing ROIs are ruled out at colliders by orders of magnitude (and may require non-perturbative couplings). This leaves three candidate operators:

- Dirac fermion DM coupling through a vector operator – $\mathcal{O}_D = (1/M_*^2)\bar{X}\gamma^\mu X\bar{q}\gamma_\mu q$
- Complex scalar DM coupling through a scalar operator – $\mathcal{O}_C = (1/M_*)\phi^*\phi\bar{q}q$
- Real scalar DM coupling through a scalar operator – $\mathcal{O}_R = (1/M_*)\phi\phi\bar{q}q$.

To address the degeneracy in determining $\{f_p, f_n\}$ from the underlying quark model, we further consider only the case where dark matter couples to the of up- and down-quarks *mass* eigenstates. While admittedly a fine-tuned scenario, this provides conservative bounds on IVDM and automatically avoids flavor constraints. In direct detection, only differences between up- and down-quark couplings produce isospin violation while contributions from other quarks are isospin-invariant. Including heavier quark contributions has no effect on the direct detection cross-section for $\mathcal{O}_D$, and generally increases the required up- and down-quark couplings for $\mathcal{O}_C$ and $\mathcal{O}_R$. However, including heavy

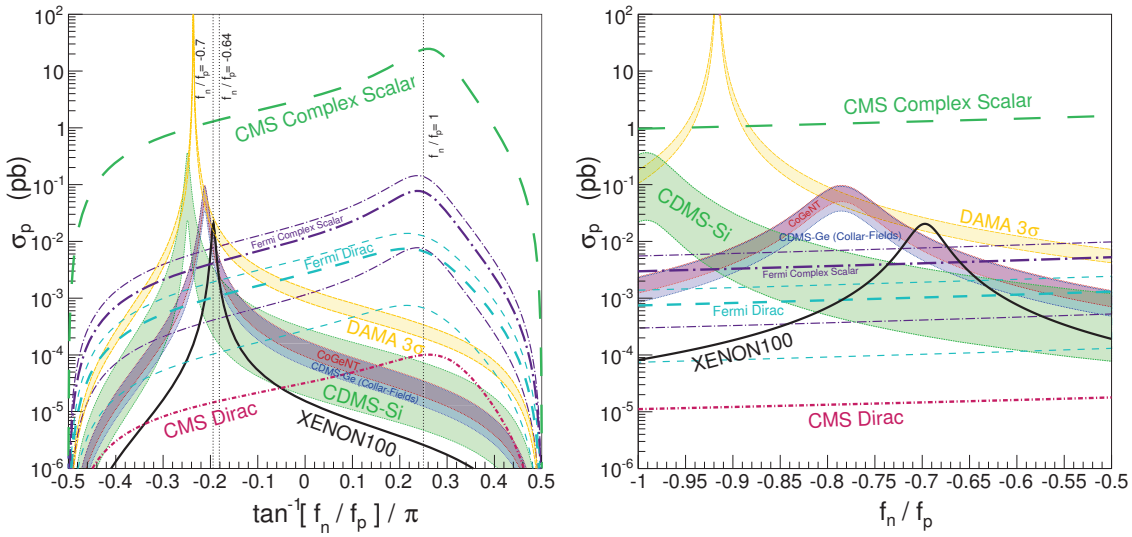

FIGURE 4. *Proton cross section for various experiments as a function of f_n/f_p for $m_X = 8$ GeV.* Plotted are slices of the 90% CL ROIs for CDMS-Si [4], CoGeNT [42], and CDMS-Ge (Collar/Fields) [23], the 3σ ROI for DAMA [1], and exclusion contours for XENON100 [10]. Also plotted are 90% CL exclusion contours for CMS [38] and for the Fermi-LAT [28], assuming DM is either a complex scalar or Dirac fermion coupling only to first generation quarks through an effective contact interaction permitting unsuppressed spin-independent scattering and *S*-wave annihilation. The thin dot-dashed violet and dashed teal lines correspond to the systematic uncertainty in the Fermi-LAT bounds from astrophysical uncertainties for complex scalar and Dirac fermion candidates, respectively.

quark contributions uniformly increases both annihilation and collider cross-sections. Depending on the operator, including couplings to heavier quarks can significantly strengthen bounds from indirect and collider searches.

Under these considerations, bounds on the annihilation cross-section were obtained from a stacked analysis of gamma ray searches from dwarf spheroidals using Fermi-LAT [27, 28]. These bounds were then translated into direct detection bounds as a function of f_n/f_p [29, 30]. These bounds are similar in strength to antiproton searches from Pamela [31, 32, 33] or Bess-Polar II [34, 35], which have been previously studied in an IVDM context [36]. However, antiproton searches but suffer from larger systematic uncertainties [37] than gamma ray searches, so we restrict our attention to Fermi-LAT bounds. Bounds were also derived from monojet searches at CMS using 4.7 fb^{-1} [38]. Simulated signal events were generated using MadGraph 5.1.5.9 [39], with showering using Pythia 6.4 [40], and detector emulation using Delphes 2.0.5 [41]. Cuts were applied according to Ref. [38], and bounds on operator strength derived from 95% CL upper limits on surviving signal events rates given therein [30].

Upper bounds from both indirect and collider searches using these criteria are relatively weak for the case of isospin-invariant dark matter, as shown in the left panel of Fig. 1. Only CMS bounds for Dirac DM provide any constraining power in the relevant parameter space region, and in this scenario the bounds are much weaker than XENON100 bounds over relevant mass ranges. CMS bounds for complex scalar DM are weaker than those for Dirac DM by five orders of magnitude, leaving the entire relevant region unconstrained. Fermi-LAT bounds are more similar for the two operators, but are also unconstraining for isospin-invariant scenarios. [1]

The constraints are significantly different in the xenophobic region. For Dirac DM in this scenario CMS bounds exclude all ROIs, and Fermi-LAT bounds partially exclude the CDMS-Si ROI and exclude the CoGeNT ROI even considering systematic uncertainties. Complex scalar bounds from Fermi-LAT are somewhat weaker, only partially excluding the CDMS-Si and CoGeNT regions, and the complex scalar collider bounds are located above the vertical axis range and are thus much too weak to provide constraining power.

The general behavior of these bounds in terms of f_n/f_p are shown in Fig. 4 for $m_X = 8$ GeV. In terms of directly constraining σ_p both CMS and Fermi-LAT limits improve by an order of magnitude in the xenophobic region relative

[1] Bounds on real scalar DM are a factor of two stronger than complex scalar DM, while bounds from CMS are a factor of two weaker.

to the isospin-invariant case. This is due destructive interference between the up- and down-quark contributions to f_p, requiring larger values of direct quark couplings required to produce the same value of f_p even without destructive interference between nucleons. However, the increase in σ_p associated with a fixed cross-section in a given direct detection experiment is much more significant, generically improving the bound relative to direct detection experiments by a factor of one hundred in the destructive interference region. This behavior is shown more clearly in Fig. 3 – the relative constraining ability of collider and indirect searches versus xenon-based experiments is improved by a factor of $\sim 10^5$ for maximal xenophobia region relative to the isospin-invariant scenario.

The bounds from indirect and collider searches are not ironclad, however. Here only operators producing s-wave annihilation were considered, and indirect bounds for operators producing only p-wave annihilation are much weaker. Most asymmetric DM models have much smaller annihilation rates in the current universe, and generally avoid indirect bounds. Both indirect and collider cross-sections are suppressed if true interactions are considered with a mediator ϕ lighter than the DM candidate, with suppression by a factor of $\sim (m_\phi/m_X)^4$. Collider bounds also depend strongly on operator dimensionality, and are much less constraining for scalars, particularly at low mass. All such model dependence is important when mapping indirect and collider search bounds into direct detection parameter space.

CONCLUSION

We have investigated scenarios with isospin-violating DM, with a focus on scenarios where DM has a suppressed coupling to xenon and thus bounds at xenon-based direct detection experiments are weakened relative to the current impressive bounds at XENON100. In this xenophobic region the tension between XENON100 and CoGeNT and CDMS-Si results are significantly reduced, and furthermore enough freedom remains to allow for overlap of the CoGeNT and CDMS-Si ROIs. On the other hand, even in the maximally xenophobic limit the ROIs reported by DAMA and CRESST remain highly constrained, and LUX will have the power to further constrain light dark matter results. We have also mapped bounds from Fermi-LAT and CMS onto the direct detection parameter space, and even with conservative choices of couplings these results have a profound impact on the xenophobic region. However, this mapping is highly model dependent, and several scenarios exist which significantly reduce the relative strength of indirect and collider bounds.

ACKNOWLEDGMENTS

We are grateful to the Center for Theoretical Underground Physics and Related Areas (CETUP* 2013) in South Dakota for its support and hospitality. We are grateful to J. Feng, J. Kumar, D. Marfatia, and L. Strigari for collaboration. DS is supported in part by U.S. Department of Energy grant DE–FG02–92ER40701 and by the Gordon and Betty Moore Foundation through Grant No. 776 to the Caltech Moore Center for Theoretical Cosmology and Physics.

REFERENCES

1. R. Bernabei, et al., *Eur.Phys.J.* **C67**, 39–49 (2010), 1002.1028.
2. C. Aalseth, et al., *Phys.Rev.Lett.* **106**, 131301 (2011), 1002.4703.
3. G. Angloher, M. Bauer, I. Bavykina, A. Bento, C. Bucci, et al., *Eur.Phys.J.* **C72**, 1971 (2012), 1109.0702.
4. R. Agnese, et al., *Phys.Rev.Lett.* (2013), 1304.4279.
5. D. Akerib, et al., *Phys.Rev.* **D82**, 122004 (2010), 1010.4290.
6. Z. Ahmed, et al., *Phys.Rev.Lett.* **106**, 131302 (2011), 1011.2482.
7. E. Armengaud, et al., *Phys.Rev.* **D86**, 051701 (2012), 1207.1815.
8. J. Angle, et al., *Phys.Rev.Lett.* **107**, 051301 (2011), 1104.3088.
9. E. Aprile, et al., *Phys.Rev.Lett.* **107**, 131302 (2011), 1104.2549.
10. E. Aprile, et al., *Phys.Rev.Lett.* **109**, 181301 (2012), 1207.5988.
11. D. Tucker-Smith, and N. Weiner, *Phys.Rev.* **D64**, 043502 (2001), hep-ph/0101138.
12. J. Collar, and D. McKinsey (2010), 1005.0838.
13. R. Bernabei, P. Belli, F. Montecchia, F. Nozzoli, F. Cappella, et al., *Eur.Phys.J.* **C53**, 205–213 (2008), 0710.0288.
14. N. Bozorgnia, G. B. Gelmini, and P. Gondolo, *JCAP* **1011**, 019 (2010), 1006.3110.
15. M. T. Frandsen, F. Kahlhoefer, C. McCabe, S. Sarkar, and K. Schmidt-Hoberg (2013), 1304.6066.
16. Y.-Y. Mao, L. E. Strigari, and R. H. Wechsler (2013), 1304.6401.
17. R. C. Cotta, A. Rajaraman, T. M. P. Tait, and A. M. Wijangco (2013), 1305.6609.

18. A. Kurylov, and M. Kamionkowski, *Phys.Rev.* **D69**, 063503 (2004), hep-ph/0307185.
19. F. Giuliani, *Phys.Rev.Lett.* **95**, 101301 (2005), hep-ph/0504157.
20. S. Chang, J. Liu, A. Pierce, N. Weiner, and I. Yavin, *JCAP* **1008**, 018 (2010), 1004.0697.
21. Z. Kang, T. Li, T. Liu, C. Tong, and J. M. Yang, *JCAP* **1101**, 028 (2011), 1008.5243.
22. J. L. Feng, J. Kumar, D. Marfatia, and D. Sanford, *Phys.Lett.* **B703**, 124–127 (2011), 1102.4331.
23. J. Collar, and N. Fields (2012), 1204.3559.
24. C. Savage, G. Gelmini, P. Gondolo, and K. Freese, *JCAP* **0904**, 010 (2009), 0808.3607.
25. C. Savage, G. Gelmini, P. Gondolo, and K. Freese, *Phys.Rev.* **D83**, 055002 (2011), 1006.0972.
26. D. Akerib, et al., *Astropart.Phys.* **45**, 34–43 (2013), 1210.4569.
27. M. Ackermann, et al., *Phys.Rev.Lett.* **107**, 241302 (2011), 1108.3546.
28. A. Geringer-Sameth, and S. M. Koushiappas, *Phys.Rev.Lett.* **107**, 241303 (2011), 1108.2914.
29. J. Kumar, D. Sanford, and L. E. Strigari, *Phys.Rev.* **D85**, 081301 (2012), 1112.4849.
30. J. L. Feng, J. Kumar, D. Marfatia, and D. Sanford (2013), 1307.1758.
31. O. Adriani, et al., *Phys.Rev.Lett.* **106**, 201101 (2011), 1103.2880.
32. Q.-H. Cao, I. Low, and G. Shaughnessy, *Phys.Lett.* **B691**, 73–76 (2010), 0912.4510.
33. J. Lavalle, *Phys.Rev.* **D82**, 081302 (2010), 1007.5253.
34. K. Abe, H. Fuke, S. Haino, T. Hams, M. Hasegawa, et al., *Phys.Rev.Lett.* **108**, 051102 (2012), 1107.6000.
35. R. Kappl, and M. W. Winkler, *Phys.Rev.* **D85**, 123522 (2012), 1110.4376.
36. H.-B. Jin, S. Miao, and Y.-F. Zhou, *Phys.Rev.* **D87**, 016012 (2013), 1207.4408.
37. C. Evoli, I. Cholis, D. Grasso, L. Maccione, and P. Ullio, *Phys.Rev.* **D85**, 123511 (2012), 1108.0664.
38. S. Chatrchyan, et al., *JHEP* **1209**, 094 (2012), 1206.5663.
39. J. Alwall, M. Herquet, F. Maltoni, O. Mattelaer, and T. Stelzer, *JHEP* **1106**, 128 (2011), 1106.0522.
40. T. Sjostrand, S. Mrenna, and P. Z. Skands, *JHEP* **0605**, 026 (2006), hep-ph/0603175.
41. S. Ovyn, X. Rouby, and V. Lemaitre (2009), 0903.2225.
42. C. Kelso, D. Hooper, and M. R. Buckley, *Phys.Rev.* **D85**, 043515 (2012), 1110.5338.